VETERINARSKI ARHIV 93 (3), 381-388, 2023 DOI: 10.24099/vet.arhiv.1731

MRI features of multiple phalangeal disorders in a draft horse – a case report

Ashraf M. Abu-Seida* and Yahya M. Elemmawy

Department of Surgery, Anesthesiology and Radiology, Faculty of Veterinary Medicine, Cairo University, Giza, Egypt

ABU-SEIDA, A. M., Y. M. ELEMMAWY: MRI features of multiple phalangeal disorders in a draft horse – a case report. Vet. arhiv 93, 381-388 2023

ABSTRACT

Magnetic resonance imaging (MRI) is fast becoming the gold standard diagnostic tool for lameness in equines. This case report describes the MRI features of multiple phalangeal disorders in a 9-year-old horse with chronic unilateral forelimb lameness due to severe trauma. A complete case history was taken, and a thorough clinical examination, radiography, ultrasonography and MRI were performed. Radiography and ultrasonography showed limited value. MRI revealed edema of the navicular bursa (NB), distal sesamoidean impar desmitis, DDFT injury at navicular and post-navicular levels, cartilage erosion of the pastern and coffin joints, medial collateral desmitis of the fetlock joint, medial collateral sesamoidean desmitis, and lateral collateral desmitis of the coffin joint. In conclusion, severe trauma may induce multiple phalangeal disorders with severe pain in draft horses, and MRI is superior to other diagnostic imaging modalities, such as radiography and ultrasonography, for diagnosing such cases.

Key words: diagnostic imaging; deep digital flexor tendon; fetlock; navicular bursa; sesamoidean ligament

Introduction

Draft horses are prone to many conditions involving lameness affecting a distal limb. Due to their large size, evaluation of lamed draft horses is a unique challenge (STECKEL, 1987).

MRI is fast becoming the gold standard diagnostic tool for musculoskeletal disorders of the distal limbs in equines, in a way that was not previously possible (MURRAY et al., 2006; MIZOBE et al., 2016; ELLIS et al., 2020; ELEMMAWY et al., 2020; ABU-SEIDA and ELEMMAWY, 2021). The use of MRI overcomes the potential disadvantages of both radiography for diagnosis of osseous lesions and ultrasonography for diagnosis of soft tissue injuries (ELEMMAWY et al., 2019). MRI has been used for diagnosis of acute ligament injuries, cartilage damage, navicular disease and fractures of navicular bone (TUNG et al., 2000; SAMPSON et al., 2008; DYSON and MURRAY, 2011).

In a recent study, MRI was used for diagnosis of both soft and osseous tissues in the fetlock and pastern regions in chronically lame draft horses (ELEMMAWY et al., 2020). Several disorders were described by MRI such as: digital tenosynovitis, straight sesamoidean desmitis, osteosclerosis in the distal part of the third metacarpal bone

*Corresponding author:
Prof. Ashraf M. Abu-Seida, Department of Surgery, Anesthesiology & Radiology, Faculty of Veterinary Medicine, Cairo University Giza - Giza Square, Egypt. PO: 12211, e-mail: ashrafseida@cu.edu.eg; ashrafseida@yahoo.com

ISSN 0372-5480
Printed in Croatia

(MCIII) or first phalanx (PI), adhesions between the straight sesamoidean ligament (SSL) and deep digital flexor tendon (DDFT), oblique sesamoidean desmitis, cartilage erosions of the fetlock or pastern joints, adhesions between the proximal digital annular ligament and DDFT, and pre-navicular DDFTendinitis (ELEMMAWY et al., 2020).

This report describes the MRI findings of multiple phalangeal injuries originating from trauma in a draft horse.

Case history

A nine-year-old draft horse was admitted to Brooke Charity Hospital, Egypt, for investigation of chronic severe right forelimb lameness due to bracing a heavy weight on a downhill road for the previous seven months. The horse received two regimens of phenylbutazone injections for 10 days without recovery. The horse had suffered from pain and lameness for seven months.

Clinical examination revealed grade 4/5 right forelimb lameness while walking, that increased with trotting to 5/5 (minimal weight bearing). The horse's phalangeal region was swollen and elicited pain on palpation. Low and high palmar perineural blocks were carried out, but there was only good improvement of the high palmar perineural block (when the medial and lateral palmar and the palmar metacarpal nerves were anesthetized slightly distally to the level of the carpometacarpal joint).

Latero-medial, dorso-palmar and skyline (for NB) radiographs of the right phalangeal region showed no osseous abnormalities.

Ultrasonography of the palmar aspect of the phalangeal region was performed using a 7.5 MHz linear transducer (Toshiba just vision, Japan) after routine preparation. Both transverse and longitudinal planes were undertaken. Ultrasound was unable to identify the confirmed lesions.

A cast was applied for 3 weeks and the horse was given flunixin meglumin (Finadyne®, MSD, Animal Health, Egypt) at a dose of 1.1mg/kg intravenously once daily for 5 days. No improvement was reported and the owner refused neurectomies. Therefore, the horse was euthanized on humane grounds at the owner's request by an overdose of I/V barbiturates due to the type of the work it did (draft horse), the chronicity of the case, its incurable lameness and the refusal of neurectomy by the owner.

Both distal forelimbs were dissected and MRI of the phalangeal region was performed. Images were obtained with a 0.3 T MR imaging system (Siemens AG 2009, Syngo MR A35, ID: 008). All images were obtained using a human brain circular coil (Tx Coil) around the center of the fetlock joint, starting from a level 10 cm proximal to the midpoint of the fetlock joint to the level of coronet distally, then re-centered at the coronet center point. The contralateral limb was imaged for comparison. The sequences and planes used are presented in Table 1.

Table 1. The parameters of MRI pulse sequences used for imaging of the phalangeal region in the examined horse

Sequence	TR(ms)	TE(ms)	Inversion Time	FA°	NEX	Echo Train Length	Slice thickness (mm)X Inter-slice spacing	Field of view	Acquisition Matrix	Time
T1 SE	1460	17	_	90	1	1	4.5 X 5.8	146*180	284*512	3:25
T2 TSE	7340	106	_	180	2	9	3 X3.3	250*250	154*192	5:23
T1 TSE Dixon	1280	34	_	90	1	1	3.5 X 4.55	250*250	144*192	2:48
T2 FS TIRM 2D	7780	22	90	180	2	7	3 X3.3	308*384	250*250	5:42

Table 1. The parameters of MRI pulse sequences used for imaging of the phalangeal region in the examined horse (continued)

Sequence	TR(ms)	TE(ms)	Inversion Time	FA°	NEX	Echo Train Length	Slice thickness (mm)X Inter-slice spacing	Field of view	Acquisition Matrix	Time
T2 FLASH 2D	542	28	_	30	2	1	4 X 4.4	183*199	246*384	4:02
T2 GE 3D	80	43	_	8	1	1	4	186*230	354*512	4:14
T1 FLASH 3D	77	17	_	14	2	1	2	244*244	176*320	6:58

R: time of repetition, TE: time of echo, FA: flip angle, SE: spin echo, FLASH: fast low angle shot, GE: gradient echo, TSE: turbo spin echo, SE: spin echo, PD: proton density.

The following MRI abnormalities were reported: an edema like lesion of the NB revealed extensive fluid based signal intensity particularly on the palmar half of the NB with no evidence of navicular bursitis on the T1 TSE Dixon sagittal images (Fig. 1a).

Distal synovial invagination into the NB showed a distended disto-palmar synovial recess of the distal interphalangeal joint (DIP) into the distal border of the NB. This invagination showed a discrete osseous cyst-like lesion (Fig. 1b).

Impar sesamoidean desmitis had increased signal intensity on all sequences. On the sagittal T1 Dixon and T2 TSE images, increased moderate signal intensity on the ligament insertion was observed (Fig. 1c). On the transverse T2 image at the level of PIII, adhesions were observed between the impar ligament and PIII and DDFT (Fig. 1d).

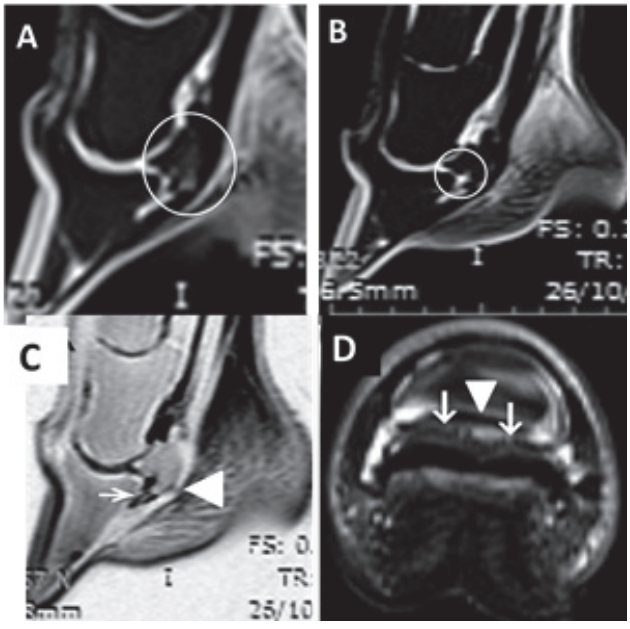

Fig. 1. (A and B) Sagittal T1 TSE Dixon image of navicular apparatus showing increased moderated signal intensity of the palmar half of the NB (White arrows) and an osseous cyst-like lesion at the distal border of the NB (circles).
(C) The sagittal PD negative image of the navicular apparatus showing the ill-distinct distal sesamoidean impar ligament (DSIL) with increased moderate signal intensity (White arrow).
(D) Transverse T2 image of DSIL showing dorsal fibrillations of the ligament, corresponding to adhesions to the palmar aspect of PIII (White arrows) and loss of palmar separation between the DSIL and the DDFT. Notice the area of low signal intensity at the palmar border of PIII (arrow head) corresponding to sclerosis.

DDFT injuries at navicular and post-navicular levels revealed high signal intensities on T1-weighted and PD sequences (Fig. 2a). On the transverse images, a palmar partial tear of the medial lobe of the DDFT was observed with inflammatory fluid of high signal intensity between the digital cushion and the DDFT (Fig. 2b).

An edema like lesion at the insertion of the DIP lateral collateral ligament demonstrated increased intermediate signal intensity at its insertion on the T1 TSE Dixon sagittal image (Fig. 2c).

The lateral collateral desmitis of the DIP showed low signal intensity of ligament origin at the distal PII on the sagittal and dorsal T1 3D GE images. On the dorsal FLASH images, a small area at the origin of the ligament showed low signal intensity (concurrent to sclerosis) compared to the medial ligament. The lateral ligament showed increased moderate signal intensity, more than the medial one. T1 3D GE and FLASH sequences were valuable for evaluation of this injury (Fig. 2d).

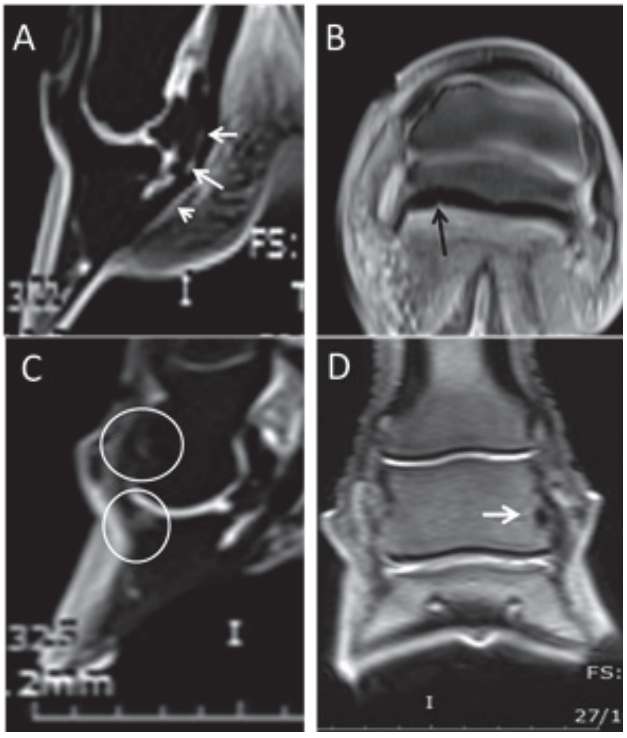

Fig. 2. (A) Sagittal T1 TSE Dixon image of the navicular apparatus showing increased moderated signal intensity dorsal to the navicular level of the DDFT (white arrows) indicating erosion of the fibrocartilaginous part of the DDFT.
(B) Transverse FLASH 3D image of the DDFT at the level of NB showing a palmar partial tear of the medial lobe of the DDFT (black arrow) and the thicker medial lobe of the DDFT than the lateral one (medial is to the left).
(C) Sagittal T1 TSE Dixon image of the lateral collateral ligament of the DIP showing increased moderate signal intensity at ligament origin and insertion (circles).
(D) Dorsal T1 3D GE image of the same ligament showing low signal intensity at ligament origin (White arrow) compared to the normal medial one (medial is to the left).

Digital tenosynovitis showed a distended digital sheath with high signal intensity at the mid-pastern region on the sagittal PD image (Fig. 3a).

Cartilage erosions of the interphalangeal joints revealed high signal intensity entrapped fluid within moderate signal intensity cartilage defects (Fig. 3b). Images of T2 TSE and T1 3D GE sequences were the most helpful images for diagnosis of cartilage erosions. Dorsal erosions of the pastern joint, and dorsal and palmar erosions of the coffin joint were noticed. The coffin joint showed greater distension than the pastern joint (4.31 mm and 2.16 mm, respectively).

On the axial T2 sequence of the medial collateral desmitis of the fetlock joint, there was a thickened ligament with low signal intensity compared to the lateral ligament. The deep part of the medial ligament was more affected than the superficial part (Fig. 3c).

Lateral collateral sesamoidean desmitis showed a thickened ligament with the increased volume of the fetlock joint synovia, and high signal intensity on the axial T2 sequence. More ligament details were observed on the FLASH sequence due to the high contrast (Fig. 3c).

The lateral extensor branch desmitis of the third interosseous muscle showed moderate high signal intensity while it passed abaxially over the lateral proximal sesamoid bone. An associated sclerotic rim with low signal intensity was noticed abaxially of the lateral proximal sesamoid bone. Subcutaneous inflammatory exudates of high signal intensity were found adjacent to both the lateral collateral sesamoidean ligament and the lateral extensor branch of the third interosseous muscle (Fig. 3c).

The medial oblique sesamoidean desmitis showed increased intermediate signal intensity along the whole ligament. The palmar aspect of the lateral oblique sesamoidean ligament showed the same abnormal MRI finding along its proximal third (Fig. 3d).

On the basis of the previous MRI findings, the primary lesion was untreated navicular disease with a DDFT tear that may have resulted in the other recorded disorders.

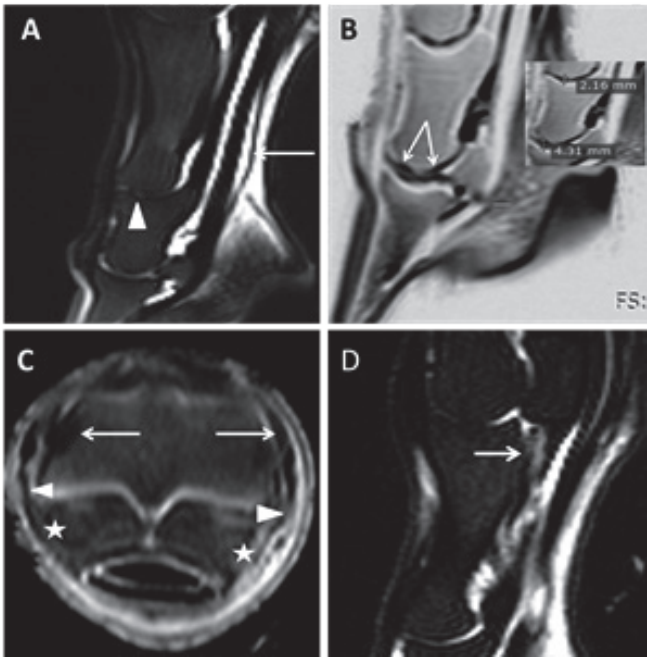

Fig. 3. (A) Sagittal T2 TSE image of the pastern joint showing two dots of low signal intensity corresponding to osteophytes with entrapped synovial fluid of increased moderate signal intensity (arrow head). Notice the distended digital sheath with high signal intensity (white arrow).
(B) Sagittal T1 3D GE negative image of the coffin joint showing the dorsal and palmar areas of cartilage loss reaching to the underlining subchondral bone (white arrows).
(C) Transverse FLASH 3D image of the fetlock joint showing the thickened medial collateral ligament, underlining sclerosis of ligament origin, and the thickened medial collateral ligament of the fetlock joint (white arrows), the thicker lateral collateral sesamoidean ligament with increased signal intensity (arrow heads), and the thickened lateral branch of the interosseous ligament with higher signal intensity (astrix, medial is to the left).
(D) Sagittal T2 image of the fetlock region showing increased moderate signal intensity along the whole length of the oblique sesamoidean ligament (OSL, white arrow).

Discussion

This report records MRI features of an unusual case of multiple injuries of traumatic origin at the phalangeal region in a draft horse. The injuries involved both soft and osseous tissues, and most of the available tools had limited diagnostic value. Therefore MRI, as the sole diagnostic tool, is highly recommended for diagnosis in similar cases.

The high number of MRI abnormalities reported in this case was attributed to the chronicity of the case. It was thought that the previous trauma might have led to navicular disease with DDFT injury at the navicular level, and proceeded to the other recorded injuries. Therefore, MRI may play a role in determining the pathogenesis of phalangeal disorders in equines.

MRI examination of 72 horses with recent navicular syndrome and normal radiographs revealed associated DDF Tendinitis, collateral sesamoidean desmitis, and impar sesamoidean

desmitis in 18%, 15% and 10%, respectively (MURRAY et al., 2006). Moreover, ELEMMAWY et al. (2020) recorded mixed digital disorders in draft horses.

Edema like lesions of the palmar half of the NB on T1 TSE Dixon sagittal images with focal accumulation dorsal to the DDFT usually reflect fibrocartilage loss. Similar findings were discussed before (MURRAY et al., 2006). No evidence of navicular bursitis was seen in this case. The relationship between navicular disease and the development of navicular bursitis is unknown (JINGFEI, 2008).

The Dixon sequence was selected to confirm the inflammatory condition in DDFT injuries and edema like lesions of the NB. The water-only image on Dixon's technique with fat suppression is widely used for diagnosis of water-based diseases in bone marrow injuries or hepatic steatosis (JINGFEI, 2008; SAMPSON et al., 2009).

Digital tenosynovitis showed high signal intensity in all MRI sequences due to the increased synovia inside the tendon sheath. This injury was thought to be a secondary non-specific lesion resulting from untreated navicular disease. This is in agreement with the findings of a previous study (MURRAY et al., 2005).

Use of fat-saturated GE and PD sequences has been found to be useful for accurate identification of articular cartilage (DISLER et al., 1995). This was the same protocol used for diagnosis of articular defects in this case. The MRI abnormalities recorded are in agreement with previous studies (DISLER et al., 1995; DYSON and DENOIX, 1995). Furthermore, the coffin joint showed a larger distension than the pastern joint, relating to the degree of erosion in each joint.

Ligaments of the fetlock region were difficult to evaluate with ultrasound due to the ergot interfering with the scan head/skin contact, and their oblique orientation. MRI provided an accurate diagnosis of oblique distal sesamoidean desmitis in this case. A similar finding was recorded in 27 horses (SAMPSON et al., 2007). Lateral collateral desmitis of the coffin joint showed low signal intensity due to sclerosis.

The novelty of this case report is the description of MRI features of multiple phalangeal disorders of traumatic origin in a draft horse, with their suspected pathogenesis. Moreover, it clarifies that MRI is superior to other diagnostic imaging modalities, such as radiography and ultrasonography, for diagnosing such cases in draft horses.

In conclusion, severe trauma may result in multiple phalangeal disorders with severe lameness in horses, and MRI is recommended for diagnosis of such cases in horses. Moreover, MRI may play a role in the detection of the pathogenesis of phalangeal disorders in horses.

Conflict of interests

Both authors declare no conflict of interest concerning the publication of this article.

References

ABU-SEIDA, A. M., Y. M. ELEMMAWY (2021): Chronic collateral sesamoidean desmopathy in draft horses: MRI and histopathological findings. J. Equine Vet. Sci. 98, 103362.
DOI: 10.1016/j.jevs.2020.103362

DISLER, D. G., T. R. MCCAULEY, C. R. WIRTH, M. D. FUCHS (1995): Detection of knee hyaline cartilage defects using fat-suppressed three-dimensional spoiled gradient-echo MR imaging: comparison with standard MR imaging and correlation with arthroscopy. AJR Am. J. Roentgenol. 165, 377-382.
DOI: 10.2214/ajr.165.2.7618561

DYSON, S., R. MURRAY (2011): The foot and Pastern. In: Equine MRI, (Murray, R. C., Ed.) Blackwell Publishing, UK, pp. 271-306.

DYSON, S. J., J. M. DENOIX (1995): Tendon, tendon sheath, and ligament injuries in the pastern. Vet. Clin. North. Am. Equine Pract. 11, 217-233.
DOI: 10.1016/S0749-0739(17)30320-6

ELLIS, K. L., M. F. BARRETT, K. T. SELBERG, D. D. FRISBIE (2020): Magnetic resonance imaging and histopathological evaluation of equine oblique sesamoidean ligaments. Equine Vet. J. 52, 522–530.
DOI: 10.1111/evj.13213

ELEMMAWY, Y. M., A. M. ABU-SEIDA, N. A. SENNA, A. F. YOUSEF (2020): MRI Features of fetlock and pastern regions in 30 chronically, un-treated lame draft horses confirmed by Postmortem examination. Int. J. Vet. Sci. 9, 217-223.
DOI:10.37422/IJVS/20.017

ELEMMAWY, Y. M., N. A. SENNA, A. M. ABU-SEIDA A. F. YOUSSEF (2019): Suspensory Branch Desmitis in a Horse: Ultrasonography, Computed Tomography, Magnetic Resonance Imaging, and Gross Postmortem Findings. J. Equine Vet. Sci. 80, DOI: 10.1016/j.jevs.2019.06.008 49-55.

JINGFEI, M. (2008): Dixon techniques for water and fat imaging. J. Magn. Reson. Imaging 28, 543-558. DOI: 10.1002/jmri.21492

MIZOBE, F., J. OKADA, Y. SHINZAKI, M. NOMURA, T. KATO, K. YAMADA, M. SPRIET (2016): Use of standing low-field magnetic resonance imaging to assess oblique distal sesamoidean ligament desmitis in three Thoroughbred racehorses. J. Vet. Med. Sci. 78, 1475–1480. DOI: 10.1292/jvms.15-0656

MURRAY, R. C., M. C. SCHRAMME, S. J. DYSON, M. V. BRANCH, T. S. BLUNDEN (2006): Magnetic resonance imaging characteristics of the foot in horses with palmar foot pain and control horses. Vet. Radiol. Ultrasound 47, 1-16. DOI: 10.1111/j.1740-8261.2005.00100.x

MURRAY, R. C., M. V. BRANCH, C. TRANQUILLE, S. WOODS (2005): Validation of magnetic resonance imaging for measurement of equine articular cartilage and subchondral bone thickness. Am. J. Vet. Res. 66, 1999-2005. DOI: 10.2460/ajvr.2005.66.1999

SAMPSON, S. N., R. K. SCHNEIDER, P. R. GAVIN, C. P. HO, R. L. TUCKER, E. M. CHARLES (2009): Magnetic resonance imaging findings in horses with recent onset navicular syndrome but without radiographic abnormalities. Vet. Radiol. Ultrasound 50, 339-346. DOI: 10.1111/j.1740-8261.2009.01547.x

SAMPSON, S. N., R. K. SCHNEIDER, P. R. GAVIN (2008): Magnetic resonance imaging findings in horses with recent and chronic bilateral forelimb lameness diagnosed as navicular syndrome. Proc. Am. Assoc. Equine Pract. 54, 419-434.

SAMPSON, S. N., R. K. SCHNEIDER, R. L. TUCKER, P. R. GAVIN, C. J. ZUBROD, C. P. HO (2007): Magnetic resonance imaging features of oblique and straight distal sesamoidean desmitis in 27 horses. Vet. Radiol. Ultrasound 48, 303-311. DOI: 10.1111/j.1740-8261.2007.00247.x

STECKEL, R. (1987): Puncture wounds, abscesses, thrush, and canker. In: Current Therapy in Equine Medicine. (Edward. R., Ed.), 2nd ed., Saunders WB, p.271.

TUNG, G.A., D. ENTZIAN, A. GREEN, J.M. BRODY (2000): High-field and low-field MR imaging of superior glenoid labral tears and associated tendon injuries. Am. J. Roentgenol. Radium Ther. 174, 1107-1114.

Received: 15 September 2021
Accepted: 19 March 2022

ABU-SEIDA, A. M., Y. M. ELEMMAWY: Značajke višestrukih falangealnih ozljeda uočene magnetskom rezonancijom (MR) u konja za vuču - prikaz slučaja. Vet. arhiv 93, 381-388 2023

SAŽETAK

Magnetska rezonancija (MR) ubrzano postaje zlatni standard u dijagnostici hromosti u konja. U ovom se radu opisuju značajke MR-a u dijagnostici višestrukih falangealnih ozljeda u devetogodišnjeg konja s kroničnom unilateralnom hromošću prednjih ekstremiteta uzrokovanom teškom traumom. Provedena je detaljna anamneza, temeljiti klinički pregled, rendgenska pretraga, ultrazvučna i MR pretraga. Rendgenska i ultrazvučna pretraga pokazale su ograničenu vrijednost. MR je otkrio edem navikularne burze (NB), distalni sezamoidni dezmitis, DDFT ozljedu na navikularnoj i postnavikularnoj razini, eroziju hrskavice putičnih i kopitnih zglobova, medijalni kolateralni dezmitis skočnog zgloba, medijalni kolateralni sezamoidni dezmitis i lateralni kolateralni dezmitis kopitnog zgloba. Zaključeno je da teška trauma može uzrokovati višestruke falangealne ozljede s jakom boli u konja za vuču, a MR je superioran ostalim metodama slikovne dijagnostike kao što su rendgenska i ultrazvučna pretraga u dijagnostici ovakvih slučajeva.

Ključne riječi: slikovna dijagnostika; tetiva dubokog sagibača prsta; skočni zglob; navikularna burza; sezamoidni ligament